# Thermoplastic Interpenetrating Polymer Networks of a Triblock Copolymer Elastomer and an Ionomeric Plastic. I. Rheology and Morphology

D. L. SIEGFRIED, D. A. THOMAS, and L. H. SPERLING, *Materials Research Center, #32, Lehigh University, Bethlehem, Pennsylvania 18015*

## Synopsis

The thermoplastic interpenetrating polymer networks (IPNs) are combinations of two physically crosslinked polymers. Thermoplastic IPNs were prepared by combining polymer I, an SEBS triblock elastomer with polymer II, an ionomer prepared from a random copolymer of styrene, methacrylic acid, and isoprene (90/10/1 by volume). Neutralization of the acid groups to form the ionomer was carried out on a Brabender Plasticorder. Two subclasses of the thermoplastic IPNs were identified. Chemically blended systems, prepared by a sequential polymerization method, were compared with compositionally equivalent mechanically blended systems prepared by melt blending the separately synthesized polymers. The chemically blended thermoplastic IPNs (CBT IPNs) exhibited lower melt viscosities than compositionally equivalent mechanically blended thermoplastic IPNs (MBT IPNs). Moreover, the melt viscosities of many of the CBT IPNs were even lower than that of either homopolymer component, leading to an explanation in terms of an unusually low value of the rubbery modulus front factor. Although both types of thermoplastic IPNs underwent a phase inversion during neutralization of polymer II, the phase inversions were often incomplete. Morphological studies revealed that more equal dual phase continuity existed in the MBT IPNs than in the CBT IPNs after ionomer formation.

## INTRODUCTION

Interpenetrating polymer networks (IPNs) have been defined as a combination of two network polymers, synthesized and/or crosslinked in the immediate presence of each other.[1-3] Employing both sequential and simultaneous modes of synthesis, these IPNs form thermosets, since both polymers are crosslinked at the completion of the reaction sequence.

While these traditional IPNs utilized covalent crosslinks, three types of noncovalent or physical crosslinks are generally recognized, including multiblock copolymers, semicrystalline polymers, and polymers bearing ionic charges. Combinations of physically crosslinked polymers, especially where both polymers attain some degree of dual phase continuity, belong to a new class of IPNs designated thermoplastic IPNs. An apparent contradiction in terms, thermoplastic IPNs describe a hybrid between a polymer blend and an IPN. These materials are thermoplastic and flow at elevated temperatures, but they behave as thermosets at use temperature.

Most recently, thermoplastic IPNs of triblock copolymers and semicrystalline polymers have been studied by Davison and Gergen.[4,5] The block copolymers were based on the triblock elastomer styrene-*b*-ethylene-*co*-butylene-*b*-styrene (SEBS), while the semicrystalline polymers are polyamides[4] or thermoplastic saturated polyesters.[5] Interpenetration of phases develops when the viscosities of the two components are nearly equal during the mechanical blending process.

Fisher[6] has developed a somewhat related thermoplastic IPN by blending partly cured EPDM rubber with semicrystalline polypropylene or polyethylene. A review of multipolymer materials which fall into the thermoplastic IPN category has been recently prepared by Kresge.[7]

All of the above examples[4-7] employ well-known mechanical blending techniques, where the polymers are synthesized separately and then combined in the melt. These materials are designated the mechanically blended thermoplastic IPNs, or MBT IPNs.

This study explores the combination of two physically crosslinked polymers prepared by polymerizing monomer II in a mutual solution with polymer I. Combination of the two polymers in this manner is designated a chemically blended thermoplastic IPN, or CBT IPN. (This material is also, technically, a graft copolymer.) The MBT IPNs and the CBT IPNs are both combinations of physically crosslinked polymers, and are both subclasses of the newly designated thermoplastic IPNs. While this study emphasizes the chemically blended materials, the corresponding mechanically blended materials were prepared for purposes of comparison.

In this investigation of thermoplastic IPNs, an SEBS triblock elastomer was combined with a random copolymer of styrene, methacrylic acid, and isoprene, SMAAI, (90/10/1 by volume). The SMAAI was subsequently neutralized with a base to form the ionomer.[8,9] The mechanical behavior of these materials was also investigated separately.[10]

## EXPERIMENTAL

### Materials

A styrene-*b*-ethylene-*co*-butylene-*b*-styrene (SEBS) triblock copolymer, designated Kraton G-1652, was obtained from the Shell Development Co. and was used as received. The SEBS had a styrene content of 29% by weight and the approximate block molecular weights: $8 \times 10^3$ g/mole, S; $39 \times 10^3$ g/mole, EB; $8 \times 10^3$ g/mole, S.[11] This material was prepared through anionic polymerization techniques to yield an unsaturated precursor, styrene-*b*-butadiene-*b*-styrene, which was subsequently hydrogenated. The final product contained less than 0.1% by weight residual unsaturation.[11]

Styrene (S) monomer was washed prior to use with 5 wt % NaOH aqueous solution to remove the inhibitor, washed with deionized water, and dried using anhydrous calcium sulfate (Drierite). Both the methacrylic acid (MAA) and isoprene (I) monomers were used as received, as was the benzoin photoinitiator. Cesium hydroxide was a 99% pure solid and sodium hydroxide was obtained as a 50% w/w aqueous solution. The antioxidant system used during melt blending operations consisted of 50% MARK 1775 (Witco Chemical Corp.), an organic phosphite, and 50% Ethyl Antioxidant 330 (Ethyl Corp.), an hindered alkylidene bisphenol.

### CBT IPN Precursors

A mutual solution of SEBS, polymer I, and the monomer mix II of S,MAA,I (90/10/1 by volume) and benzoin (0.4% w/v) was effected and subsequently photopolymerized in the presence of near UV fluorescent light for 72 hr. The

incorporation of 1% isoprene in polymer II permitted staining with osmium tetroxide to improve phase contrast for electron microscopy.

Concentrations of SEBS in the solution ranged from 25 to 75 wt %. For a 25 wt % solution, the syrupy mixture was poured between two clamped glass plates separated by a Viton rubber gasket and photopolymerized to yield the IPN precursor. The IPN precursor, as used here, defines polymer II in the acid state.

To prepare compositions containing more than 25 wt % SEBS, mutual solution was achieved by placing the required amounts of polymer I and monomer II in a closed petri dish, allowing imbibing of monomer II by SEBS to proceed in a darkened dessicator for 24 hr, and finally photopolymerizing the viscous mixture in the closed petri dish.

## MBT IPN Precursors

The monomer mixture of S,MAA,I (90/10/1 by volume) and benzoin (0.4% w/v) was photopolymerized between two clamped glass plates separated by a Viton rubber gasket for 72 hr. The resulting terpolymer, SMAAI, was melt blended with SEBS in a Brabender Plasticorder Torque Rheometer to produce the MBT IPN precursor, as described below.

## Melt Blending and Neutralization Procedures

A Brabender Plasticorder Torque Rheometer was employed to process the IPN precursors and thermoplastic IPNs and determine their dynamic flow properties. Both shear rate and mixing temperature were controlled. Typically, a 42-g sample was processed at 50 rpm for about 30–40 min at 180–185°C. After chemical changes within the polymer sample ceased, an equilibrium torque (in m g) was recorded on the Plasticorder. Melt viscosity data was reported in torque for convenience, however, torque values can be converted to absolute viscosity via relationships established by Goodrich and Porter[12] (e.g., at 50 rpm, multiplication of the torque in m g by nine yields the melt viscosity in P; multiplication by 0.9 gives melt viscosity in Pa sec).

In the case of the CBT IPNs, the material was first melt blended as synthesized. For the mechanically blended analogs, the separately prepared materials were melt blended together to form a macroscopically homogeneous mass. Again, both of these materials, before neutralization, are designated as IPN precursors, since the SMAAI does not yet contain physical crosslinks.

As the IPN precursor fused, 1 wt % of the antioxidant system was added to the polymer melt.

After an equilibrium torque was recorded (within 15 min), the neutralization of the MAA mers was carried out using a 10% aqueous alkali solution (either NaOH or CsOH). The stoichiometric or substoichiometric amount of base required to neutralize all or part of the acid groups was calculated based on the known composition of the IPN precursor. The aqueous alkali solutions were added dropwise from a pipette through the mixer opening while the mixing operation continued. The water flashed off as steam from the hot melt leaving a finely divided alkaline material which readily neutralized the MAA mers.[8,9]

During the neutralization reaction, the melt viscosity of the nascent thermo-

plastic IPN increased. Mixing continued at constant temperature for at least 10 min after the addition of the alkali solution to assure completion of the neutralization reaction and thorough mixing of the newly formed thermoplastic IPN. When the new and consequently higher equilibrium torque was established, Brabender processing was halted, and the thermoplastic IPN melt was removed and cooled to ambient temperatures. Initial (before neutralization) and final torque values were recorded.

A typical Brabender Plasticorder data curve illustrating changes in torque during the various processing stages is shown in Figure 1. High initial torque values were recorded prior to complete fusion of the material. After neutralization was completed, a torque somewhat higher than the final equilibrium torque was recorded (see the Results section).

For subsequent mechanical[10] and morphological studies, compression-molded sheets were formed at 180°C under 6 MPa of platen pressure for 5 min in a molding press.

When the composition of a CBT IPN is designated, two numbers representing the relative percents of polymer I and polymer II are separated by a slash (e.g., 50/50), whereas the use of a plus sign denotes the composition of the mechanically blended counterpart (e.g., 50 + 50).

## Molecular Weight of Polymer II

In order to determine the molecular weight of polymer II in the IPN precursor, samples of a 50/50 composition and a 50 + 50 composition (both in acid form and processed at 180°C for 30 min on the Brabender) were dissolved in a toluene/methanol (90/10 by volume) solvent mixture. The final concentration of polymer was 10%. Two-layer films formed after solvent evaporation. The bottom layer (polymer II) was redissolved in toluene/methanol (90/10 by volume), and its intrinsic viscosity $[\eta]$ was determined in a Cannon-Ubbelhode semimicro dilution-type viscometer. The viscosity-average molecular weights $M_v$ were calculated using the Mark–Houwink relation $[\eta] = KM_v^a$.[13] The value of $a$ used in the Mark–Houwink relation was 0.715, and the value of $K$ was $1.04 \times 10^{-2}$ ml/g.

The value of $M_v$ for polymer II was higher in the CBT IPN precursor ($3.4 \times 10^5$ g/mole) than in the MBT IPN precursor ($1.7 \times 10^5$ g/mole). This might be
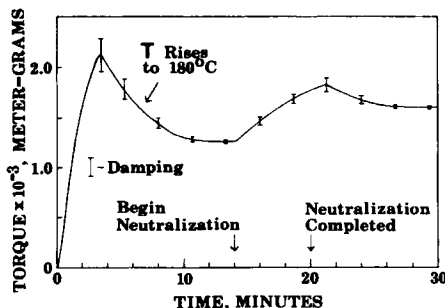


Fig. 1. Brabender Plasticorder torque vs. time for a 50/50 SEBS/SMAAI CBT IPN processed at 50 rpm and 180°C and neutralized with aqueous NaOH solution. Damping indicates normal fluctuations in torque recorded by Plasticorder. The initial "rise" in the torque results from melt fracture of cold samples.

expected because of the Trommsdorf effect existing during formation of the CBT IPN precursor. For comparison, the $M_v$ value of polymer II, as polymerized, was $2.4 \times 10^5$ g/mole.

## Transmission Electron Microscopy (TEM)

Two staining techniques were utilized to increase the electron density of the SMAAI polymer II phase. The first method was based on Kato's osmium tetroxide staining technique.[14] Specimens with cross sections of $0.2 \times 0.2$ mm and lengths ranging from 2 to 10 mm were exposed to osmium tetroxide vapor at room temperature for one week in order to selectively stain the residual double bonds of the isoprene mers. The second procedure involved neutralization of the MAA groups with cesium hydroxide instead of sodium hydroxide. Cesium's greater electron density provided phase contrast for the ionomer and also had been used by other investigators[15–19] with success. No observable differences in properties were noted when $Cs^+$ was substituted for $Na^+$.

Portions of the stained specimens were embedded in an epoxy resin, trimmed to a truncated pyramid shape, and microtomed on a porter Blum MT-2 ultramicrotome using a diamond knife.[20] Ultrathin sectioning at room temperature to a thickness of 60–80 nm (600–800 Å) yielded satisfactory results. Transmission electron micrographs were taken employing a Philips 300 electron microscope.

## RESULTS

### Rheological Behavior

Torque data presented in Table I were obtained for the various thermoplastic IPN compositions and homopolymers at a shear rate of 50 rpm and a processing temperature of 180°C, except where noted. In general, the homopolymers and higher elastomer compositions required a slightly higher temperature for proper melt flow to occur.

Initial torques represent the equilibrium torques attained prior to addition of aqueous base to the polymer melts. The final torques represent the new equilibrium torques after conversion of polymer II to the ionomer (see Fig. 1).

For the homopolymer SMAAI, all of the acid groups were neutralized to form the ionomer as was done for the IPNs. For the triblock copolymer SEBS, no aqueous base was added, but the SEBS was processed for 30 min to note any changes in torque due to processing at 185°C.

Control samples for various two-polymer compositions processed for 30 min with no aqueous base addition revealed increases of less than 10% in torque. Control samples also provided the IPN precursors needed for morphological studies and mechanical testing.[10]

When CBT IPN precursors were compared with MBT IPN precursors of the same overall composition, initial torque values were generally very similar. However, after neutralization to form the ionomer, the final torque values for the MBT IPNs were significantly higher than those for corresponding CBT IPNs of the same composition, as noted in Table I. The disparity became greater as the percent ionomer in the IPN increased. Since the melt rheology of a two-

TABLE I

Changes in Torque Associated with 100% Neutralization of Polymer II MAA mers to Form
Thermoplastic IPNs

| Material | Alkali | Torque (m g) | | Percent change |
| | | Initial | Final | |
|---|---|---|---|---|
| | | CBT IPNs–SEBS/SMAAI | | |
| 75/25 | CsOH | 1375[a] | 1525[a] | 11 |
| 50/50 | NaOH | 1265 | 1600 | 26 |
| 50/50 | CsOH | 1200 | 1600 | 33 |
| 35/65 | NaOH | 1125 | 1525 | 36 |
| 35/65 | CsOH | 1150 | 1550 | 35 |
| 25/75 | NaOH | 1340 | 1925 | 44 |
| 25/75 | CsOH | 1410 | 1975 | 40 |
| | | MBT IPNs–SEBS + SMAAI | | |
| 75 + 25 | NaOH | 1400[a] | 2025[a] | 45 |
| 50 + 50 | NaOH | 1265 | 2050 | 62 |
| 35 + 65 | NaOH | 1025 | 2065 | 101 |
| 25 + 75 | NaOH | 1100 | 3225 | 193 |
| | | Homopolymers | | |
| SMAAI | NaOH | 1175[a] | 4400[a] | 275 |
| SEBS | — | 2020[a] | 2020[a] | 0 |

[a] Determined at 185°C.

phased composition depends on its morphology, this rheological finding suggested that important morphological differences existed between CBT and MBT IPNs.

## Partial Neutralization

Examination of the relative torque values for the homopolymers showed that the acid form of SMAAI had a lower viscosity than the SEBS, but the ionomer form of SMAAI had a higher viscosity than the SEBS. This reversal in relative viscosities of polymer I and polymer II implies that an inversion in relative phase continuities may have occurred during formation of the ionomer in the IPN. Then the SMAAI would be expected to be more continuous in the IPN precursor and the SEBS more continuous in the final IPN. Furthermore, at some intermediate neutralization stage, a situation was postulated to exist where the viscosities of the two polymers were equivalent, and dual phase continuity would exist. Further neutralization would result in a phase inversion.

Rheological data presented in Table II for the partial neutralizations of the 50/50 SEBS/SMAAI CBT IPNs shows the increasing percent change in torque as percent neutralization increases.

During Brabender processing (see Fig. 1), a somewhat higher torque than the final equilibrium torque was recorded immediately after neutralization was completed. This rheological feature may be associated with the phase inversion process.

Processing conditions for 50/50 and 50 + 50 compositions were also varied to observe the effect of increased processing shear rate and temperature on the rheology and morphology. Rheological data are listed in Table III. As the shear

TABLE II
Changes in Torque Associated with Increasing Percent Neutralization of 50/50 SEBS/SMAAI
CBT IPNs

| Percent neutralization | Alkali | Torque (m g) | | Percent change |
|---|---|---|---|---|
| | | Initial | Final | |
| 0 | — | 1250 | 1265 | 1 |
| 15 | CsOH | 1325 | 1400 | 6 |
| 25 | CsOH | 1325 | 1400 | 6 |
| 50 | CsOH | 1125 | 1270 | 13 |
| 100 | NaOH | 1265 | 1600 | 26 |
| 100 | CsOH | 1200 | 1600 | 33 |

rate is increased from 50 to 150 rpm, the percent increase in torque on neutralization decreased significantly for both CBT and MBT IPNs. However, increasing the temperature alone had a much smaller effect.

In summary, the percent increase in torque was less with the CBT IPNs than with the MBT IPNs processed at the same temperature and shear rate.

## Rheological Data Analysis

Since phase inversion and/or cocontinuity are of prime importance, the rheological data demands further analysis. Many equations have been derived to predict the properties of two-phase mixtures. The Hashin–Shtrikman equations[21-23] predict a lower bound [eq. (1)] and an upper bound [eq. (2)] for the viscosity $\eta_M$ of non-Newtonian fluid mixtures consisting of one phase dispersed in the other phase:

$$\text{lower bound:} \quad \eta_M = \eta_I + \frac{v_{II}}{1/(\eta_{II} - \eta_I) + v_I/2\eta_I} \tag{1}$$

$$\text{upper bound:} \quad \eta_M = \eta_{II} + \frac{v_I}{(1/\eta_I - \eta_{II}) + v_{II}/2\eta_{II}} \tag{2}$$

TABLE III
Changes in Torque Associated with 100% Neutralization of Polymer II MAA mers with CsOH:
Variations in Processing Shear Rate and Temperature

| rpm | $T$ (°C) | Torque (m g) | | Percent change |
|---|---|---|---|---|
| | | Initial | Final | |
| CBT IPNs–50/50 SEBS/SMAAI | | | | |
| 50 | 180 | 1200 | 1600 | 33 |
| 50 | 200 | 1150 | 1440 | 25 |
| 150 | 200 | 1100 | 1250 | 14 |
| MBT IPNs–50 + 50 SEBS + SMAAI | | | | |
| 50 | 180 | 1265 | 2050 | 62[a] |
| 150 | 180 | 1190 | 1725 | 41 |
| 50 | 200 | 990 | 1675 | 69 |
| 150 | 200 | 1075 | 1350 | 26 |

[a] From Table I, for comparison.

The symbols $\eta_I$ and $\eta_{II}$ represent the experimentally determined melt viscosities of polymers I and II, respectively, and $v_I$ and $v_{II}$ equal the respective volume fractions, where the $v_I + v_{II} = 1$.

Also, an inverse rule of mixtures, eq. (3), has been used[23,24] to predict $\eta_M$ assuming a morphology of many concentric layers of polymer I in polymer II:

$$\eta_M = (W_I/\eta_I + W_{II}/\eta_{II})^{-1} \qquad (3)$$

The weight fractions for polymers I and II are represented by $W_I$ and $W_{II}$, respectively, where $W_I + W_{II} = 1$.

Experimentally determined torque values for the several compositions are compared with the above theoretical predictions in Figure 2 for the thermoplastic IPN precursors and in Figure 3 for the thermoplastic IPNs. Most of the torque data for the IPN precursors lie below the theoretical curves, with little difference between CBT and MBT IPN precursors. At higher polymer II contents, the viscosity of the mixtures is lower than that of either component, except for the 25/75 chemically blended products which are higher than predicted.

Torque data for the thermoplastic IPNs in Figure 3 reveal that the MBT IPNs have lower viscosities than predicted. Moreover, the CBT IPNs exhibit much lower viscosities than predicted, even lower than the viscosity of SEBS. A molecular and phenomenological interpretation of this behavior will be presented in the discussion.

## Morphological Characteristics

The morphological changes induced by neutralization of the MAA mers in polymer II were investigated by examining stained specimens of both acid and salt forms of the CBT and MBT IPNs using transmission electron microscopy
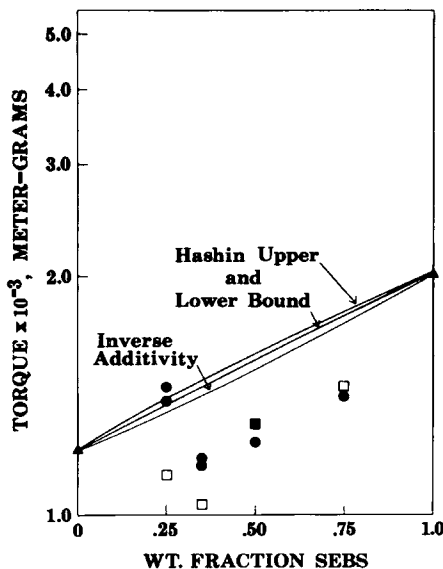


Fig. 2. Comparison of experimental torque data for the IPN precursors with the Hashin lower and upper bound predictions and the inverse additivity prediction. (□) Mechanical blends; (●) chemical blends; (▲) homopolymers.
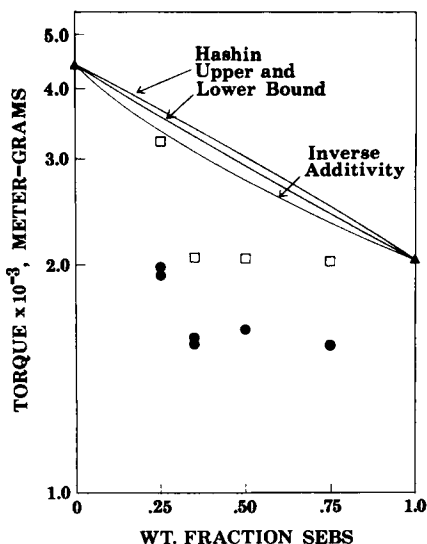
Fig. 3. Comparison of experimental torque data for the thermoplastic IPNs with the Hashin lower and upper bound predictions and the inverse additivity prediction. Symbols as in Fig. 2.

(TEM). In all cases, polymer II was preferentially stained with either osmium, cesium, or osmium plus cesium, as indicated. (It was established that the $Cs^+$ and $OsO_4$ staining agents attacked the same phase in all cases.)

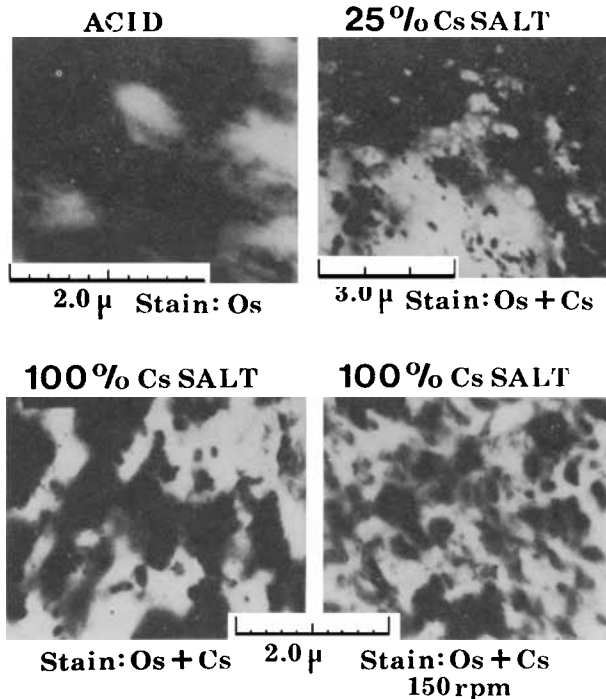Micrographs presented in Figure 4 illustrate the sequence of microscopic



Fig. 4. Morphologies of 50/50 CBT IPNs. All samples processed at 50 rpm, except where noted. Staining technique indicated under each micrograph.

structural changes which occurred during the processing and neutralization of a 50/50 CBT IPN. The IPN precursor (acid form) in Figure 4, upper left, exhibited a more continuous (darker) SMAAI phase with two levels of mixing: a coarser cellular structure with 100–200 nm (0.1–0.2 $\mu$m) dimensions and a finer intrastructure on the order of 10–30 nm (100–300 Å). Finding a more continuous polymer II structure confirmed that it was the less viscous component.

The lower left micrograph in Figure 4 illustrates that a sample neutralized 100% contains a dispersed polymer II phase (100–200 nm) often appearing as "composite droplets."[21,25] Some polymer I appears to have been engulfed by polymer II during the phase inversion.

When neutralization of 25% of the MAA mers by cesium hydroxide was carried out, a partial phase inversion was observed. As shown in Figure 4, upper right, portions of this composition possessed more continuous SEBS phase structures, portions existed where SMAAI was clearly more continuous, and intermediate transitional regions were found where dual phase continuity existed.

It should be noted that a partial phase inversion was also detected by TEM at 15% neutralization, but that at 50% neutralization the inversion was apparently complete, polymer II being dispersed in a more continuous polymer I matrix.

Processing at the higher shear rate of 150 rpm (Fig. 4, lower right) tends to elongate and smear the segregated polymer II regions. This micrograph reveals the flow patterns followed by polymer II during processing of the melt.

It is interesting to contrast the morphology of a CBT IPN with that of the corresponding MBT IPN. Composite Figure 5 contains micrographs for 50 +
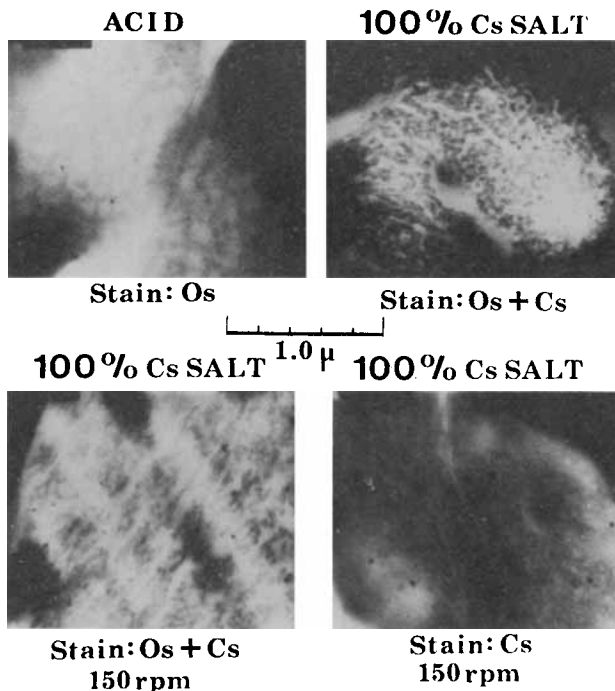


Fig. 5. Morphologies of 50 + 50 MBT IPNs. Samples processed at 50 rpm, except where noted. Staining technique indicated under each micrograph.

50 compositions before and after ionomer formation.   In the acid state (Fig. 5, upper left), polymer II (SMAAI) is more continuous in space, as would be expected, since the melt viscosity of SMAAI is lower than that of SEBS.   Polymer I forms a cellular structure 80–150 nm (800–1500 Å) in diameter; however, the cell contents are relatively stain-free, indicating less extensive mixing has occurred compared to the corresponding CBT IPN precursor.

Upon neutralization (Fig. 5, upper right), polymer I becomes the more continuous phase with islands of the more viscous polymer II dispersed throughout the polymer I matrix.   These islands are often elongated with dimensions ranging from 500 nm (0.5 $\mu$m) to 2000 nm (2.0 $\mu$m); however, most islands are interconnected at some point, and not completely dispersed.   In addition, each island consists of smaller (40–100 nm) connected domains of polymer II interdispersed throughout the polymer I.

Individual islands of polymer II can be described as collapsed cell wall structures containing concomitant decreased cellular contents of polymer I.   Postulation of a contraction mechanism occurring for polymer II during ionomer formation would seem to be consistent with the cocontinuous nature of the semi-dispersed polymer II islands.   Figure 5 shows that these islands of cocontinuous phases can be further broken up if the Brabender shear rate is increased to 150 rpm (Fig. 5, lower left and lower right), although the dispersity does not approach that of a 50/50 CBT IPN.   The lower two micrographs in Figure 5 also confirm that both cesium and osmium stain the same locations in space.

Figure 6 shows a unique morphology reminiscent of "rabbit footprints in the snow" for the cesium salt of a 25/75 CBT IPN.   Oriented flow patterns have been preserved from the melt, and some aspects of dual phase continuity exist where many of the polymer II regions are connected.
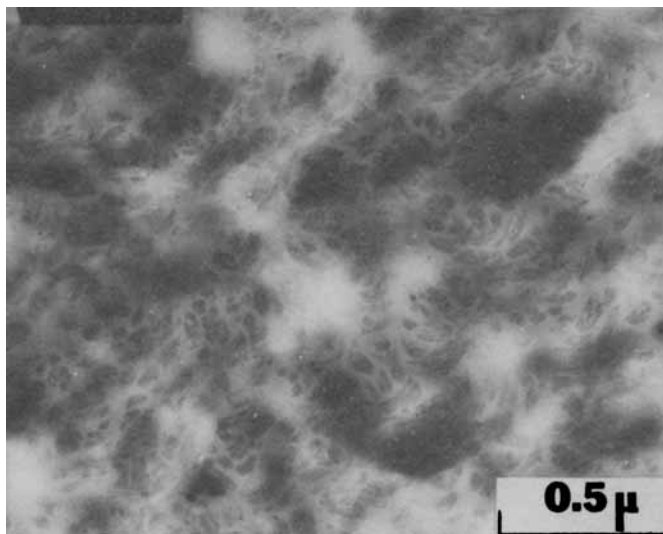


Fig. 6. Morphology of a 25/75 CBT IPN.   Neutralization was with CsOH; polymer II was also stained with osmium tetroxide.

## DISCUSSION

Classically, the IPNs were defined as a combination of two network polymers having been synthesized and/or crosslinked in the immediate presence of each other.[1-3] While covalent crosslinks were intended, physical crosslinks can also be used, and form the basis for the thermoplastic IPNs.

The CBT IPNs also constitute a type of graft copolymer. In this sense, a graft copolymer is defined as the polymerization of monomer II in the immediate presence of polymer I, regardless of the extent of actual graft formation.[26] As considered previously, a graft copolymer becomes an IPN when the number of deliberately introduced crosslink sites exceeds the number of (accidently introduced) graft sites, and/or the morphology and concomitant physical properties are seriously altered by the presence of the crosslinks.

As described above, the present thermoplastic IPNs are a hybrid-type material, exhibiting, it is hoped, the better features of both polymer blends and IPNs. These materials flow and are processable at elevated temperatures, yet they are "thermoset" at use temperatures.

### Phase Continuity Diagram

In general, the polymer with the higher concentration or the lower viscosity tends to form the continuous phase. At nearly equal viscosities and/or weight fractions some aspects of dual phase continuity may be initiated. Transmission electron microscopy revealed important information regarding phase continuity as a function of percent neutralization of the MAA mers and composition of the thermoplastic IPNs. Adapting a format reminiscent of Avgeropoulos et al.,[27] the TEM results for CBT IPNs were plotted in Figure 7, which represents a generalized "phase continuity" diagram. The demarcations for the different phase continuity regions serve only to approximate where changes in phase continuity occur.

Many of the CBT IPN compositions, although phase inverted, were shown
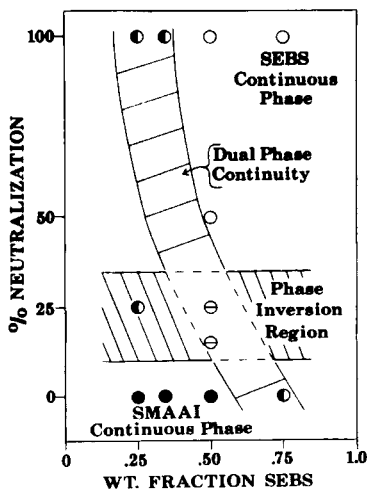


Fig. 7. Phase continuity of CBT IPNs as a function of percent neutralization of the MAA mers and composition. Electron microscopy results: (O) SEBS continuous; (●) SMAAI continuous; (◐) dual phase continuity; (⊖) phase inversion.

to retain some degree of dual phase continuity. This indicates that the phase inversion remained somewhat incomplete, probably because of the relatively equal melt viscosities of the two polymers, before and after neutralization of the MAA mers.

### Influence of SEBS Phase Domain Structure

Examination of the solubility parameters[13] listed in Table IV suggests that three distinct phases should exist in the IPN precursor materials. Determining the molecular orientation of the various phases and the nature of the interfacial boundaries between phases, however, requires speculative reasoning.[28-31]

Surfactant action by the styrene endblocks seem plausible since the styrene endblock domain diameter of 10–30 nm (100–300 Å)[32] is considerably smaller than the 100- to 200-nm ionomer phase sizes in a 50/50 CBT IPN. The existence of some mutual compatibility between polymer II and the styrene endblocks, developed through the common styrene mers, would be anticipated to result in increased surfactant action by the styrene endblocks on the polymer II phase. In a CBT IPN, the *in situ* polymerization of monomer II takes place preferentially in the vicinity of the styrene endblocks, as indicated by relative solubility parameters (Table IV). This maximizes the interfacial interaction between the partially compatible styrene endblocks and polymer II.

The resulting surfactant action, coupled with the persistence of the domain structure of the triblock copolymer in the melt,[4,33-39] suggests that the CBT IPNs well-mixed phase structure is preserved during melt processing. As neutralization of the MAA mers proceeds, the domain structure of polymer I is postulated to control the dispersion of the more viscous polymer II during the phase inversion, effectively behaving like mobile crosslinks which restrict the size of the dispersed phase.[40]

This same maintenance of SEBS domain structure in the melt, however, would prevent the nascent MBT IPN from achieving the same intimacy of mixing found in the CBT IPN. As a result, interfacial interaction of styrene endblocks with polymer II would not be as great, and during the phase inversion process resulting from ionomer formation, not as much control of ionomer phase size could be exerted by the physical crosslinks of polymer I. Thus, the ionomer phase may remain highly interconnected, due to resistance of breakdown domain structure of polymer I in the melt.

The inherent difference in phase inversion mechanisms for the two types of

TABLE IV
Solubility Parameters for Monomers and IPN Precursor Components

|  | $\delta(J/m^3)^{1/2} \times 10^{-3}$ |
| --- | --- |
| styrene monomer | 19.0 |
| methacrylic acid monomer | 22.9 |
| isoprene monomer | 15.1 |
| poly(ethylene-co-butylene) block | 16.2 |
| polystyrene block | 18.6 |
| poly(styrene-co-methacrylic acid) | 19.4–21.7 |
| (90% styrene/10% methacrylic acid) | |

IPNs, as discerned from TEM results, probably arises from the extensive mixing found in a CBT IPN precursor versus the coarser cellular structure of polymer II associated with the MBT IPN precursor. Consequently, a more cocontinuous phase structure results in the MBT IPN.

### Molecular and Phenomenological Interpretation

The abnormally low melt viscosities shown in Figure 3 have a counterpart in the solid state, as presented in the following paper on mechanical behavior.[10] The rubbery modulus of a 75/25 CBT IPN was also abnormally low. The polymerization of polymer II *in situ* was postulated to have a profound effect on the end-to-end distance of the EB portion of the triblock elastomer. Although mutual solution of polymer I and monomer II might be expected to increase the end-to-end distance of the EB molecule, through rearrangement effects the end-to-end distance is postulated to return nearly to its unperturbed dimensions. After polymerization of monomer II and concomitant phase separation, the quantity $\bar{r}_i^2$ is predicted to decrease proportional to the $\frac{2}{3}$ power of the inverse of the volume increase on swelling.

As a result, the front factor $\bar{r}_i^2/\bar{r}_f^2$,[41-43] in the modulus equation

$$E = 3(\bar{r}_i^2/\bar{r}_f^2)nRT \qquad (4)$$

would be decreased below unity, thus accounting for the anomalously low modulus of the 75/25 CBT IPN. In eq. (4), $n$ represents the number of moles of network chains per cm$^3$ and $R$ and $T$ stand for the gas constant and absolute temperature, respectively. In the front factor $\bar{r}_i^2/\bar{r}_f^2$, $r_i$ and $r_f$ are the end-to-end distances of the network chains and free chains, respectively.

Noting that the melt viscosity $\eta$ of a polymer can be related to its modulus through the equation[44]

$$\eta = \frac{1}{3}\tau E \qquad (5)$$

where $\tau$ is the characteristic relaxation time, it might be possible to extend the applicability of the front factor theory to the melt state of CBT IPNs. Thus, consideration of the end-to-end distance between physical crosslinks of SEBS in a CBT IPN might provide an explanation for their unusually low melt viscosities compared to the mechanically blended analogs and the component homopolymers.

Anomalously low melt viscosities for polymer blends have also been observed elsewhere.[21,45,46] Reasons for the occurrence of polymer blend melt viscosities lower than that of either constituent have not been conclusively established. Speculation centers on the effects of internal circulation of the dispersed phase in a shear field, and the possible storage of elastic energy by the dispersed, deformable phase with a resulting lower apparent viscosity for the blend.[21,45,46] Indeed, Han and co-workers[45,46] have found that for mechanical blends of polystyrene and high-density polyethylene, the blend which had the lower viscosity also exhibited the higher elasticity.

## CONCLUSIONS

The chemical blending of a triblock copolymer elastomer with an ionomeric plastic produced a thermoplastic IPN exhibiting a significantly lower melt viscosity than the mechanically blended analog. Morphological studies revealed that more equal dual phase continuity existed in the MBT IPNs than in the CBT IPNs after ionomer formation, this being consistent with the MBT IPNs higher melt viscosity.

Both types of thermoplastic IPNs underwent a phase inversion during neutralization of the MAA mers; however, the phase inversions were often incomplete and of a different form, thus yielding different morphologies. Apparently, more extensive surfactant action between styrene endblocks and polymer II takes place in the well-mixed phase structure of the CBT IPN precursor, thus promoting greater dispersity of the ionomer during the phase inversion. Thus, it is hypothesized that the phase domain structure of SEBS retained in the melt plays a major role in the development of various morphologies.

It was postulated that a reduced end-to-end distance between physical crosslinks of SEBS in the CBT IPNs compared to the SEBS homopolymer might account for their anomalously low melt viscosities.

In the above, reference is made to "equal" and "unequal" dual phase continuity. The scientific literature adequately defines materials having a continuous and a discontinuous phase. Although less work has been done in the area of two equally continuous phases, the term is generally understood.

However, it is also possible to have unequally cocontinuous phases. Although each phase exhibits some degree of macroscopic continually, it would be easier for a Maxwell demon to traverse the material within one of the phases. Analytical expressions describing the several families of such cases are virtually nonexistent, hampering the analysis of the rheological data in Figures 2 and 3.

## References

1. L. H. Sperling, *J. Polym. Sci. Macromol. Rev.*, **12**, 141 (1977).
2. S. C. Kim, D. Klempner, K. C. Frisch, N. Radigan, and H. L. Frisch, *Macromolecules*, **9**, 258 (1976).
3. Y. S. Lipatov and L. M. Sergeeva, *Russ. Chem. Rev.* (Engl. Transl.), **45**(1), 63 (1976).
4. S. Davison and W. P. Gergen, U.S. Pat. 4,041,103 (1977).
5. W. P. Gergen and S. Davison, U.S. Pat. 4,101,605 (1978).
6. W. K. Fischer, U.S. Pat. 3,806,558 (1974).
7. E. N. Kresge, in *Polymer Blends*, D. R. Paul and S. Newman, Eds., Academic, New York, 1978, Vol. 2, chap. 20.
8. R. W. Rees, U.S. Pat. 3,264,272 (1966); and 3,404,134 (1968).
9. R. W. Rees, in *Polyelectrolytes*, K. C. Frisch, D. Klempner, and A. V. Patsis, Eds., Technomic, Westport, CT, 1976.
10. D. L. Siegfried, D. A. Thomas, and L. H. Sperling, *Polym. Eng. Sci.*, to appear.
11. Geoff Holden, Shell Chemical Co., private communication, 24 July 1979.
12. J. E. Goodrich and R. S. Porter, *Polym. Eng. Sci.*, **7**(1), 45 (1967).
13. *Polymer Handbook*, 2nd ed., J. Brandup and E. H. Immergut, Eds., Wiley-Interscience, New York, 1975, Chap. IV.

14. K. Kato, *Jpn. Plast.,* **2,** 6(1968).

15. R. Longworth, in *Ionic Polymers,* L. Holliday, Ed., Halstead, Wiley, New York, 1975, chap. II.

16. A. Eisenberg and M. King, *Ion Containing Polymers: Physical Properties and Structure,* Academic, New York, 1977.

17. S. C. Hargest, J. A. Manson, and L. H. Sperling, *J. Appl. Polym. Sci.,* **25,** 469 (1980).

18. P. J. Phillips, *J. Polym. Sci. Polym. Lett. Ed.,* **10,** 443 (1972).

19. D. L. Siegfried, D. A. Thomas, and L. H. Sperling, *J. Appl. Polym. Sci.,* **26,** 141 (1981).

20. M. Matsuo, T. K. Kwei, D. Klempner, and H. L. Frisch, *Polym. Eng. Sci.,* **10,** 327 (1970).

21. H. Van Oene, in *Polymer Blends,* D. R. Paul and S. Newman, Eds., Academic, New York, 1978, Vol. 1, chap. 7.

22. Z. Hashin and S. Shtrikman, *J. Mech. Phys. Solids,* **11,** 127 (1963).

23. L. E. Nielsen, *Predicting the Properties of Mixtures: Mixture Rules in Science and Engineering,* Marcel Dekker, New York, 1978.

24. R. F. Heitmiller, R. Z. Maar, and H. H. Zabusky, *J. Appl. Polym. Sci.,* **8,** 873 (1964).

25. H. Van Oene, *J. Colloid Interface Sci.,* **40,** 448 (1972).

26. J. A. Manson and L. H. Sperling, *Polymer Blends and Composites,* Plenum, New York, 1976.

27. G. N. Avgeropoulos, F. C. Weissert, P. H. Biddison, and G. G. A. Bohm, *Rubber Chem. Technol.,* **49,** 93 (1976).

28. S. L. Aggarwal, *Polymer,* **17,** 938 (1976).

29. S. L. Aggarwal and R. A. Livigni, *Polym. Eng. Sci.,* **17,** 498 (1977).

30. T. Inoue, T. Soen, T. Hashimoto, and H. Kawai, in *Block Polymers,* S. L. Aggarwal, Ed., Plenum, New York, 1970, pp. 53–79.

31. T. Inoue, T. Soen, T. Hashimoto, and H. Kawai, *Macromolecules,* **3,** 87 (1970).

32. J. F. Beecher, L. Marker, R. D. Bradford, and S. L. Aggarwal, *J. Polym. Sci., Part C,* **26,** 117 (1969).

33. G. Holden, E. T. Bishop, and N. R. Legge, *J. Polym. Sci., Part C,* **26,** 37 (1969).

34. G. Holden, in *Recent Advances in Polymer Blends, Grafts, and Blocks,* L. H. Sperling, Ed., Plenum, New York, 1974.

35. G. Krause and J. T. Gruver, *J. Appl. Polym. Sci.,* **11,** 2121 (1967).

36. D. F. Leary and M. C. Williams, *J. Polym. Sci. Polym. Phys. Ed.,* **11,** 345 (1973); **12,** 265 (1974).

37. C. P. Henderson and M. C. Williams, *J. Polym. Sci., Polym. Lett. Ed.,* **17,** 257 (1979).

38. C. I. Chung and J. C. Gale, *J. Polym. Sci. Polym. Phys. Ed.,* **14,** 1149 (1976).

39. C. I. Chung and I. L. Lin, *J. Polym. Sci. Polym. Phys. Ed.,* **16,** 545 (1978).

40. T. Nishi, T. K. Kwei, and T. T. Wang, *J. Appl. Phys.,* **46,** 4157 (1975).

41. A. V. Tobolsky and M. C. Shen, *J. Appl. Phys.,* **37,** 1952 (1966).

42. M. C. Shen, T. Y. Chen, E. H. Cirlin, and H. M. Gebard, in *Polymer Networks: Structure and Mechanical Properties,* A. J. Chompff and S. Newman, Eds., Plenum, New York, 1971.

43. D. L. Siegfried, D. A. Thomas, and L. H. Sperling, *Macromolecules,* **12,** 586 (1979).

44. J. D. Ferry, *Viscoelastic Properties of Polymers,* 2nd ed., Wiley, New York, 1970.

45. C. D. Han and Y. W. Kim, *Trans. Soc. Rheol.,* **19,** 245 (1975).

46. C. D. Han, *Rheology in Polymer Processing,* Academic, New York, 1976, chap. 7.